The Penetration by Sulfur of NiO Scales Growing on Nickel

M. C. Pope* and N. Birks†

The transport of sulfur through growing scales may occur by chemical (solution and diffusion) or physical (gas molecule permeation) mechanisms. Both possibilities are examined theoretically for the case of NiO growing on nickel. Experiments are designed and carried out to establish which mechanism plays the major role in sulfur transport. The results indicate that the physical mechanism is likely to be predominant.

INTRODUCTION

Although there is little doubt that sulfur dissolves substantially in metal oxides[1-10] and that sulfur can penetrate growing oxide layers during high-temperature oxidation, there is still room for discussion about the mechanism by which such transport of sulfur is achieved.

The two major possibilities for transport of sulfur appear to be (1) dissolution and diffusion at a lattice constituent and (2) transport as the gas species, SO_2 molecules, down microcracks, grain boundaries, or disolcation pipes. These are not to be viewed as alternatives, but as mechanisms that may both proceed in parallel. The only question is which mechanism predominates.

In the case of the attack of alloys, particularly stabilized stainless steels, by carbonaceous gases there is substantial evidence[11,12] of penetration of carbon through the scale, to be incorporated into the metal phase,

*British Steel Corporation, Ladgate Lane, Middlesbrough, England.
†Department of Metallurgy, Sheffield University, England.

eventually precipitating as carbides. In this case, with scales consisting of iron oxides of very low solubility for carbon, estimated[13] to be less than 10^{-5} wt.% at 750°C for wustite, the solution and diffusion mechanism can be discounted. The alternative mechanism of migration of gas molecules through defects in the scales was proposed by Fujii and Meussner[14] and Birks.[15]

The transport of gas molecules through major scales has been substantiated by Rahmel,[16] who explains increased reaction rates in the presence of carbonaceous gases and water vapor by the action of a gaseous redox system in the cracks and pores of a growing scale. Further, Manenc[17] has shown that if an iron–carbon alloy is oxidized to produce a compact adherent oxide scale, carbon is not removed from the metal but instead shows enrichment in the surface layers as scaling proceeds.

The presence of physical defects in growing scales is evident from the work of Bruce and Hancock.[18–20]

Chang et al.[21] have investigated the diffusion of sulfur 35 with single and polycrystalline samples of both NiO and CoO at 1000–1100°C in air and established that sulfur in solution can diffuse quite rapidly through the solvent oxide. The diffusion coefficient was reduced by doping the oxide with Cr_2O_3, thereby increasing the concentration of nickel vacancies and thus decreasing the concentration of anion vacancies. Chang et al.[22] also found that the diffusivity of sulfur increased as the equilibrium oxygen partial pressure was decreased. These two results indicate that sulfur may migrate through the solvent oxide via anion vacancies.

In view of the existence of evidence for both types of transport of third elements through scales, a series of experiments was carried out to determine which mechanism predominates in the case of the transport of sulfur through growing NiO scales at 1000°C.

Theory

The dissolution of sulfur in, and its transport through, an oxide scale can occur only when the sulfur partial pressure at the scale–gas interface is higher than that at the metal–scale interface. More important, such transport cannot result in sulfide formation at the metal–scale interface unless the sulfur partial pressure eventually achieved there is above the decomposition pressure of the sulfide.

If the sulfur partial pressure at the scale–gas interface is p''_{S_2} and at the metal–scale interface is p'_{S_2}, then transport through the oxide by a dissolution mechanism can occur only if

$$p''_{S_2} > p'_{S_2} \tag{1}$$

If the formation of a metal sulfide is represented by

$$m A + \tfrac{1}{2} S_2 = A_m S; \qquad \Delta G_2^0 \tag{2}$$
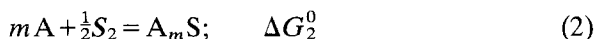
then penetration of an oxide scale can lead to formation of $A_m S$ only if

$$p_{S_2}'' > (1/a_A^{2m}) \exp(2\Delta G_2^0/RT) \tag{3}$$

For pure metals sulfide formation at the metal–scale interface can occur only if

$$p_{S_2}'' > \exp(2\Delta G_2^0/RT) \tag{4}$$

This condition, in the case of a growing oxide layer on a pure metal, can be represented on a stability diagram as shown in Fig. 1. The condition of Eq. (4) occurs only in that part of the oxide ($A_n O$) phase field lying above the extrapolated boundary between the metal (A) and sulfide ($A_m S$) phase fields, represented as a cross-hatched area. Atmospheres belonging to this area can be produced by equilibrating CO–CO_2–SO_2 mixtures.

In the case of sulfur transport occurring by SO_2 molecules permeating through the oxide scale from the atmosphere to the metal–scale interface, the effect of the local oxygen partial pressure imposed on the sulfur dioxide decomposition equilibrium must be considered.

The equilibrium between oxygen, sulfur, and sulfur dioxide is represented by

$$\tfrac{1}{2} S_2 + O_2 = SO_2; \qquad \Delta G_5^0 = -364{,}000 + 72.6 \text{ TJ} \tag{5}$$
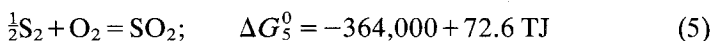
From Eq. (5) the sulfur partial pressure developed at any site is given by

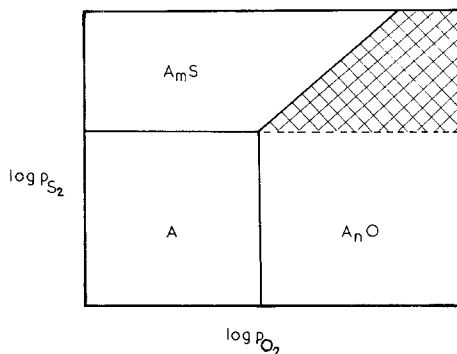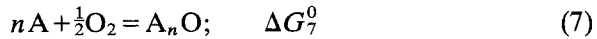$$p_{S_2} = (p_{SO_2}/p_{O_2})^2 \exp(2\Delta G_5^0/RT) \tag{6}$$

Fig. 1. Metal–sulfide–oxide phase diagram.

Within the scale the local oxygen partial pressure is imposed by the local metal activity and the equilibrium

$$n A + \tfrac{1}{2} O_2 = A_n O; \qquad \Delta G_7^0 \tag{7}$$

from which

$$p_{O_2} = (1/a_A^{2n}) \exp(2 \Delta G_7^0 / RT) \tag{8}$$

substituting Eq. (8) in Eq. (6):

$$p_{S_2} = p_{SO_2}^2 a_A^{4n} \exp[2(\Delta G_5^0 - 2 \Delta G_7^0)/RT] \tag{9}$$

If the metal sulfide $A_m S$ forms by Eq. (2), then sulfide may form at any place where the sulfur potential developed is high enough, i.e., exceeds that resulting from the equilibrium of reaction (2):

$$p_{S_2}^+ = (1/a_A^{2m}) \exp(2 \Delta G_2^0 / RT) \tag{10}$$

Combining Eqs. (9), (10), and (11), it is clear that sulfide may form at any place within the scale where the condition

$$p_{S_2} > p_{S_2}^+ \tag{11}$$

i.e.,

$$p_{SO_2} a_A^{(2m+n)} \exp[(\Delta G_5^0 - 2 \Delta G_7^0 - \Delta G_2^0)/RT] > 1 \tag{12}$$

is found.

It is also clear from Eq. (12) that the most likely conditions for sulfide formation arise when the values p_{SO_2} and a_A are at their highest. This condition is found at the metal–scale interface where $a_A = 1$, assuming that the value p_{SO_2} reaches its value in the atmosphere.

Alternatively, rearranging Eq. (13), sulfide may form at the metal–scale interface if

$$p_{SO_2} > \exp[(\Delta G_2^0 + 2 \Delta G_7^0 - \Delta G_5^0)/RT] \tag{13}$$

Experimental

At 1000°C sulfidation of nickel leads to formation of a liquid sulfide phase; due to the lack of thermodynamic data it is not possible to construct a phase diagram such as Fig. 1 for this temperature. Instead the sulfide–oxide boundary has to be determined experimentally. To do this NiO samples were exposed to atmospheres as indicated in Fig. 2. The atmosphere compositions were known quite accurately according to the good agreement between calculated[23] and measured oxygen partial pressures. After exposure the samples were analyzed for sulfur and also examined by
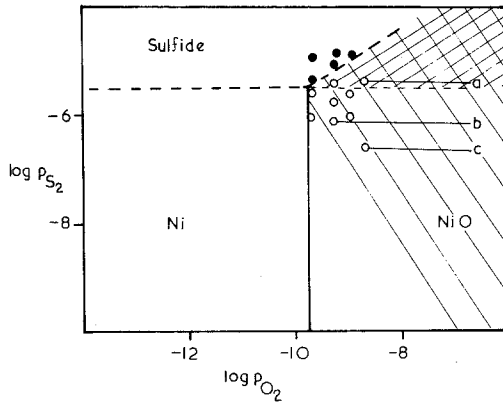
Fig. 2. Ni–nickel sulfide–NiO phase diagram at 1000°C.

X-ray diffraction. Those samples that persisted in gaining sulfur with time without equilibrating and showed evidence of sulfide diffraction lines are indicated by closed circles in Fig. 2, where open circles indicate conditions under which the NiO samples equilibrated and showed NiO lines only. The oxide–sulfide boundary line has accordingly been drawn in intersecting the Ni phase field at $p_{S_2} = 2.8 \times 10^{-6}$.

In Fig. 2 the phase boundaries have been indicated by dotted lines. except for the Ni–NiO boundary, which is known with some accuracy. Accordingly if a nickel specimen on which an oxide layer is growing is exposed to atmospheres in the cross-hatched region of the NiO phase field then any sulfur penetration may be by diffusion or permeation. Penetration on exposure to atmospheres in the singly-hatched region could have resulted only from gaseous permeation of sulfur through the oxide layer. The lower limit of P_{SO_2} at which penetration leading to sulfide formation at the metal–scale interface may be possible was calculated using Eqs. (9) and (11), putting $a_A = 1$,

$$p_{SO_2}^2 \exp[2(\Delta G_5^0 - 2\Delta G_7^0)/RT] > 2.8 \times 10^{-6} \tag{14}$$

or, rearranging, when

$$p_{SO_2} > 1.67 \times 10^{-3} \exp[(2\Delta G_7^0 - \Delta G_5^0)/RT] \tag{15}$$

substituting for ΔG_5^0 and ΔG_7^0 at 1000°C, Eq. (15) reduces to

$$p_{SO_2} > 0.04 \text{ atm.}$$

Thus, penetration of an oxide layer by SO_2 leading to a concentration of SO_2 greater than 4% being established at the metal–scale interface is likely

to lead to sulfide formation there. Generally this condition is expected to occur when the SO_2 partial pressure in the atmosphere exceeds 4%. This condition has been taken to define the limit of the singly-hatched area in Fig. 2.

Nickel specimens were oxidized at 1000°C in pure oxygen to produce a uniform oxide layer 12 μ thick in about 2 hr. A scale 50 μ thick could be produced in about 50 hr. Cross-section metallographic examination and SEM examination of the oxidized surface confirmed that the oxide completely covered the metal surface and was uniform and compact. The scale thickness was therefore calculated from the observed weight gain recorded using an automatic recording balance.

When the desired scale thickness was developed, the atmosphere was changed for a mixture of CO and CO_2 corresponding to a selected point of the NiO field of the equilibrium diagram of Fig. 2. The specimen was then exposed to this atmosphere for about 2 hr; the scale developed at this stage is shown in Fig. 3.

Finally SO_2 was admitted to the reaction chamber using a capillary injector[24] and the subsequent reaction followed by observing the weight gain with time.

The atmospheres used in these experiments are indicated in Fig. 2 and had the following compositions: (a) $CO/CO_2 = 2 \times 10^{-3}$, $p_{SO_2} = 0.5$ atm lying in the cross-hatched area, (b) $CO/CO_2 = 4 \times 10^{-3}$, $p_{SO_2} = 0.05$ atm, and ((c) $CO/CO_2 = 2 \times 10^{-3}$, $p_{SO_2} = 0.12$ atm. Both (b) and (c) were in the singly-hatched area, i.e., in the molecular-transport region.

When SO_2 was admitted to the oxidizing CO/CO_2 atmosphere, in all cases there was a period of 8–10 min during which the reaction rate was unaltered. After about 10 min the specimen began to gain weight rapidly. These experiments were terminated after various times, and the surfaces were examined by SEM. Those specimens exposed for short times showed a smooth, flat, unblemished gray scale surface; those exposed for longer times, up to 70 hr, showed the development of surface blisters. The initial 10 min period probably corresponds to establishment of equilibrium in the gas phase and time required to SO_2 to diffuse to the metal–scale surface.
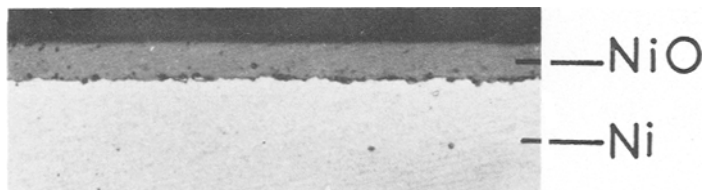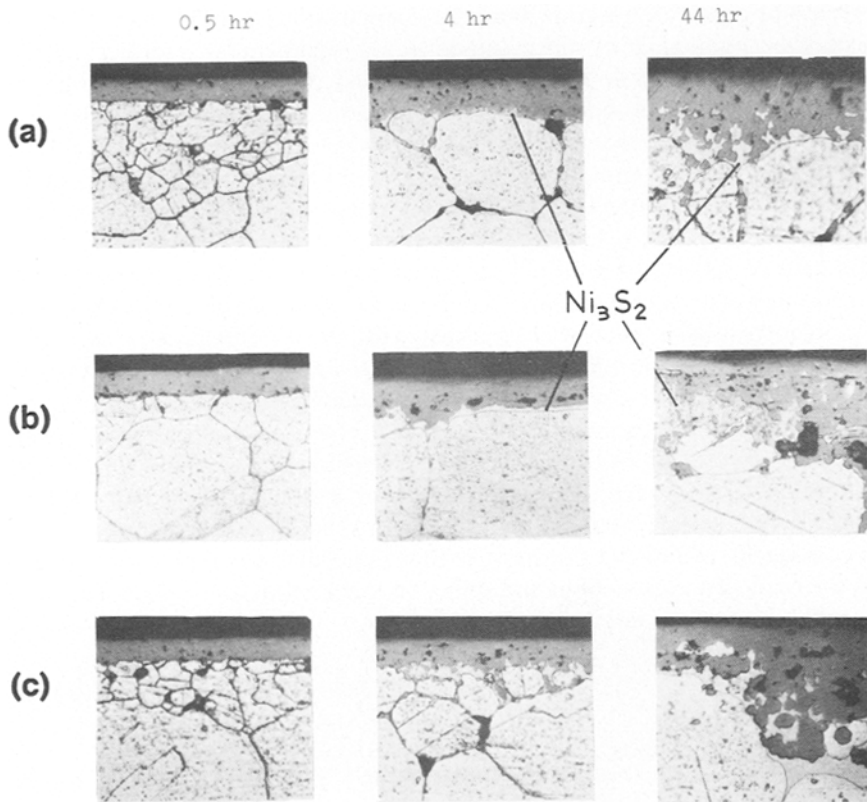

Fig. 3. Preformed oxide scale on nickel. 1.5 hr preoxidation, 1000°C ×480.

Fig. 4. Metallographic features of Ni–scale interface after sulfur penetration through preformed oxide. Etched in Merica's reagent. (a) $CO/CO_2 = 2 \times 10^{-3}$; $p_{SO_2} = 0.5$ atm. (b) $CO/CO_2 = 4 \times 10^{-3}$; $p_{SO_2} = 0.05$ atm. (c) $CO/CO_2 = 2 \times 10^{-3}$; $p_{SO_2} = 0.12$ atm.

Metallographic observation of polished cross sections of scale revealed that the same structure developed in all three cases. These are shown in Fig. 4 because both lattice diffusion and molecular transport mechanisms are possible for atmosphere (a), but only molecular transport is possible for atmospheres (b) and (c). The similarity in the modes of attack in all three cases indicates that the transport of SO_2 molecules through physical defects in the growing oxide scale is the predominant transport mechanism for sulfur under these conditions.

Figure 4 includes micrographs of specimens exposed to the three atmospheres for 0.5, 4, and 44 hr after initial oxide formation. The samples were etched in Merica's reagent to emphasize the sulfide phase. After 0.5 hr exposure to the SO_2, sulfide has begun to form at the scale–metal interface; the etch has also outlined the grain boundaries in the metal.

After 4 hr considerable grain-boundary penetration by sulfide has occurred with the appearance of more sulfide at the scale–metal interface. After 44 hr large areas of liquid eutectic are found in the original metal grain boundaries, together with globular oxide particles that have possibly precipitated from an oxide-containing eutectic during cooling.

Increasing the preformed oxide layer thickness from 12μ to 60μ increased the incubation period from 10 min to about 100 min when SO_2 was introduced. The resulting reaction rates were also much slower than in the case of specimens with a 12μ preoxidized scale. The penetration of sulfur, however, although slower, follows the same pattern in both cases.

The results of this work contrast with those of Alcock et al.[5] and Wootton,[26] who reported that preoxidation scale thicknesses of 0.2μ were sufficient to prevent attack by SO_2 penetration. The present results were obtained using atmospheres of controlled oxygen and sulfur partial pressures corresponding to quite high nickel activities, which may explain the difference. This aspect is now being pursued, although the present results indicate quite clearly that the penetration of growing oxide scales by sulfur is easily achieved by the transport of SO_2 molecules down physical defects in the scale. The dissolution and diffusion mechanism may also operate in parallel, but it does not predominate.

REFERENCES

1. M. C. Pope and N. Birks, *Oxid. Met.* **12**, 191 (1978).
2. V. N. Konev, V. N. Chebotin, N. V. Suntsov, and L. I. Statseva, *Zashch. Met.* **6**, 448 (1970).
3. M. R. Wootton and N. Birks, *Corros. Sci.* **12**, 829 (1972).
4. H. C. Chao, Y. E. Smith, and L. H. Van Vlack, *Trans. Am. Inst. Min. Metall. Pet. Eng.* **227**, 796 (1963).
5. G. R. St. Pierre and J. Chipman, *Trans. Am. Inst. Min. Metall. Pet. Eng.* **206**, 700 (1968).
6. R. A. Sharma and F. D. Richardson, *Trans. Am. Inst. Min. Metall. Pet. Eng.* **233**, 1586 (1965).
7. G. J. W. Kor and F. D. Richardson, *Trans. Inst. Min. Met. London*, **79**, C148 (1970).
8. G. J. W. Kor and F. D. Richardson, *J. Iron Steel Inst., London*, **206**, 700 (1968).
9. G. J. W. Kor, *Metall. Trans.* **3**, 2343 (1972).
10. G. J. W. Kor and E. T. Turkdogan, *Metall. Trans.* **2**, 1571 (1971).
11. H. E. McCoy, *Corrosion* **21**, 84 (1965).
12. W. B. Jepson, J. E. Antill, and J. B. Warburton, *Br. Corros. J.* **1**, 15 (1965).
13. H. Meurer and H. Schmalzried, *Arch. Eisenhuettenwes.* **42**, 87 (1971).
14. C. T. Fujii and R. A. Meussner, *J. Electrochem. Soc.* **114**, 435 (1967).
15. N. Birks, *Br. Corros. J.* **3**, 56 (1968).
16. A. Rahmel, *Werkst. Korros.* **16**, 837 (1956).
17. J. Manenc, J. Band, and J. P. Plumensi, *Werkst. Korros.* **23**, 876 (1972).
18. D. Bruce and P. Hancock, *J. Inst. Met.* **97**, 140, 148 (1969).
19. D. Bruce and P. Hancock, *J. Iron Steel Inst.* **208**, 1021 (1970).
20. P. Hancock, *Werkst. Korros.* **21**, 1002 (1970).
21. R. H. Chang, W. Stewart, and J. B. Wagner, Jr., "Reactivity of Solids," Proceedings of the 7th International Symposium, Bristol, July 1972, p. 231.

22. D. R. Chang, R. Nemoto, and J. B. Wagner Jr., *Metall. Trans.* **7A**, 803 (1976).
23. M. C. Pope, J. H. Woodhead, and N. Birks, to be published.
24. T. Flatley and N. Birks, *J. Iron Steel Inst.* **209**, 523 (1971).
25. C. B. Alcock, M. G. Hocking, and S. Zador, *Corros. Sci.* **9**, 111 (1969).
26. M. R. Wootton, Ph.D. thesis, Sheffield University (1971).